Entry-prohibited effect of KHz pulsed magnetic field upon interaction between SPIO nanoparticles and mesenchymal stem cells

Peng Wang, Siyu Ma, Guangfu Ning, Wu Chen, Bin Wang, Dewen Ye, Bo Chen, Yuzhi Yang, Qing, Jiang, Ning Gu*, Jianfei Sun*.

Abstract*—*Objective: **The interaction between superparamagnetic iron oxide (SPIO) nanoparticles and mesenchymal stem cells (MSCs) in the presence of pulsed magnetic field (PMF) has become important areas of research in recent years.** ***Methods:*** **A parameter-adjustable pulsed magnetic field was developed based on the principle of insulated gate bipolar translator (IGBT) transistor-controlled discharge of large capacitances. The internalizations of SPIO nanoparticles by MSCs were investigated under the treatment of PMF in both intermittent stimulation mode and continuous stimulation mode.** ***Results:*** **The intensities and frequencies of pulsed magnetic field can be adjustable in the range of 1.9-4.6mT and 3-5 kHz, respectively. This PMF was safe to the MSCs. However, the uptake of SPIO nanoparticles by MSCs was significantly prohibited under the treatment of KHz-ranged PMF while the 10Hz PMF enhanced the cellular uptake of nanoparticles. This phenomenon was relative with the magnetic effect of the PMF with different frequency.** ***Conclusion:*** **The PMF can be used to effectively regulate the cellular uptake of SPIO nanoparticles and the mechanism lies in the magnetic effect.** ***Significance:*** **The interaction between SPIO nanoparticles and the MSCs is a fundamental and important issue for nanomedicine and stem cell research. Our results demonstrated the external magnetic field can be used to regulate their interaction. We believed that this safe, facile and flexible method will greatly promote the development and clinical translation of regenerative medicine and nanomedicine.**

***Index Terms*—Pulsed magnetic field; Mesenchymal stem cells; Magnetic nanoparticles; Cellular internalization;Regulation**

This work is supported by grants from the National Basic Research Program of China (2017YFA0104301) and National Natural Science Foundation of China (NSFC, 81802135). (Peng Wang and Siyu Ma contributed equally to this work.) (Corresponding author: Ning Gu and Jianfei Sun.)

Peng Wang, Siyu Ma, Bin Wang, Yuzhi Yang and Qing Jiang are with the Drum Tower Hospital affiliated to Medical School of Nanjing University, Zhongshan Road 321, Nanjing, 210008, P. R. China.

Bo Chen is with the Materials Science and Devices Institute, Suzhou University of Science and Technology, 1 Kerui Road, Suzhou, Jiangsu 215009, P. R. China.

Dewen Ye, Ning Gu (correspondence e-mail: guning@seu.edu.cn) and Jianfei Sun (correspondence e-mail: sunzaghi@seu.edu.cn) are with the State Key Laboratory of Bioelectronics and Jiangsu Key Laboratory of Biomaterials and Devices, School of Biological Sciences and Medical Engineering, Southeast University, Dingjiaqiao 87, Nanjing, 210009, P. R. China.

Guangfu Ning and Wu Chen are with the Jiangsu Key Laboratory of Smart Grid Technology and Equipment, School of Electrical Engineering, Southeast University, Sipailou 2, Nanjing, 210096, P. R. China.

I. INTRODUCTION

Mesenchymal stem cells (MSCs) have obtained a great amount of attention in regenerative medicine and tissue engineering because of the capacity to differentiate into multiple types of adult cells [1]. Because of the multipotent differentiation and paracrine capability, stem cells are regarded as an innovative technology that can change the current paradigm of medicine. However, this technology is in its infant period. There remain amounts of critical issues to clarify, such as controllable homing, mimicking the niches *in vivo* and fate regulation [2][3][4]. Here, biomaterials are often involved in these issues. Recently, superparamagnetic iron oxide (SPIO) nanomaterials get increasing attentions in fundamental research and practical application of stem cells because the nano iron oxide is the only inorganic nanomaterial approved by FDA as nanodrug. It can be remotely controlled by magnetic field and has been used as the clinical MRI contrast agent[5][6][7]. This nanomaterial will play an important role in the fundamental research and the practical application of stem cells, such as production, tracing and delivery[8][9]. For example, it is an inevitable issue in clinic to trace the migration and fate of stem cells after implantation *in vivo*[10]. The SPIO nanoparticles here can be used as the MRI tracer to non-invasively monitor the stem cells[11]. However, the presence of SPIO nanoparticles may bring about some effects upon the stem cells. For example, there were some reports about the transmembrane entry of SPIO nanoparticles into the cells, which can trigger cascaded cellular responses to influence the behaviors of stem cells[12][13][14]. In addition, the cell phenotype and particularly the differentiation capacity affected by SPIO nanoparticles have also been widely studied. For example, in some cases, SPIO-labeled mesenchymal stem cells showed marked inhibition of chondrogenesis but not adipogenesis or osteogenesis[15]. Magnetic nanoparticles can also be beneficial to mesenchymal stem cells differentiation for cartilage repair [16]. The magnetism of SPIO nanoparticles can also be used to force magnetically the stem cells towards a given differenciation pathway, such as the cardiac route[17]. Thus, interaction between the SPIO nanoparticles and the stem cells is the fundamental issue for the clinical translation of stem-cells research. The entry of nanoparticles into cells is a primary approach for nanoparticles to interact with cells. Commonly, the stem cells are labeled with SPIO nanoparticles via co-incubation method. Due to the intrinsic magnetism, there have been numerous reports about magnetic field to boost the entry of SPIO nanoparticles into the cells, which mechanism lies in

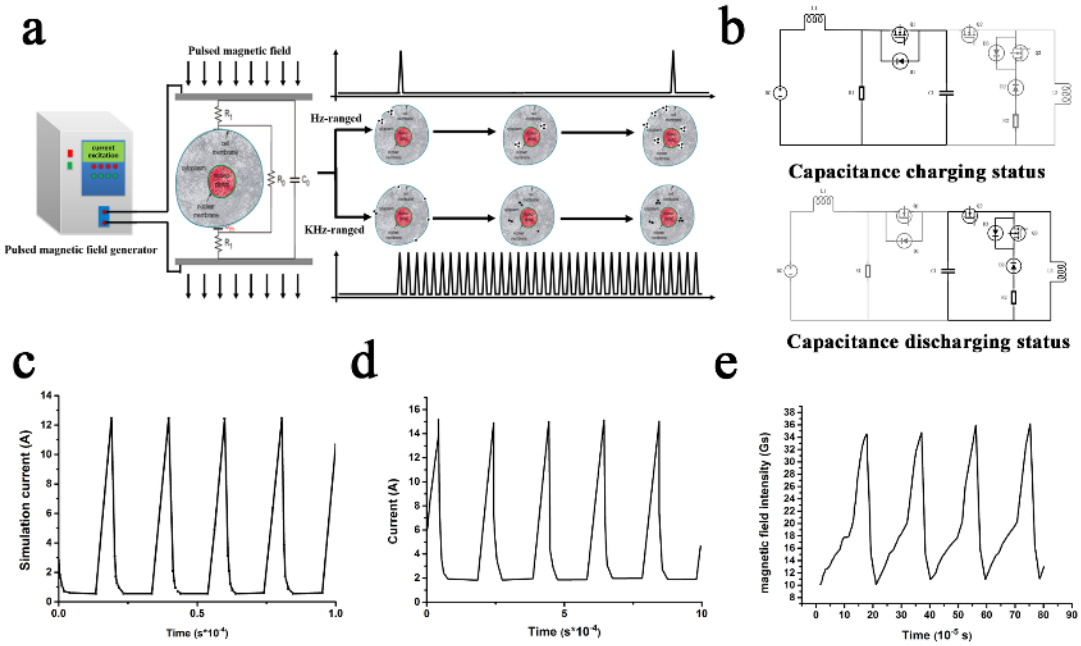

Figure. 1 (a) Schematic showing the systems of the PMF and its influencing mechanism on cellular internalization of SPIO nanoparticles. (b) The circuit layout of PMF, describing the generation of the pulsed current consist of capacitance charging status and capacitance discharging status. (c) The simulated output wave profile of the PMF. (d) the measured pulsed current waveform by current clamp. (e) The measured output intensity of PMF by high-frequency Tesla-meter.

the force effect[18][19]. Meanwhile, pulsed magnetic field (PMF) was also employed to assist the transmemebrane entry of SPIO nanoparticles[20][21]. Generally, the field intensity was higher than 0.1T and the frequency was lower than 100Hz. However, the high intensity of PMF drew safety concerns[22]. More importantly, the force-actuated transmembrane process of nanoparticles may be essentially different from that in the co-incubation. The latter mainly results from the spontaneous endocytosis[23].

With a viewpoint of electronic component, a cell can be regarded as a capacitance[24]. Hence, the cell is conductive when it is subjected to an electromagnetic field of high frequency, which means charged carriers can easily pass through a cell. Therefore, it is an interesting issue for the entry of SPIO nanoparticles into stem cells in the presence of a high-frequency PMF. Unfortunately, this issue remains lacking of investigation which is partly by reason that the PMF of high frequency has not been extensively applied in biomedical fields. In this study, a PMF generator was designed and produced which intensity and frequency can beadjusted in the range of 1.9-4.6mT and 3-5 kHz, respectively. Then a type of CFDA-approved SPIO nanoparticles were co-incubated with the MSCs, during which period the cells were periodically treated with the PMF. It was discovered that the 3 and 5 kHz PMF can effectively prohibit the uptake of SPIO nanoparticles by MSCs while the 10Hz PMF enhanced the cellular uptake of nanoparticles. By comparing with experimental results those from Au nanoparticles, the influence resulting from the magneto-electrical induction was excluded, indicating that the critical influential causes of PMF on cellular internalization of nanoparticles lies in the magnetic effects. This novel phenomenon is beneficial to regulation of interaction between magnetic nanoparticles and stem cells with an external field. Furthermore, these results can contribute to the elucidation of a critical scientific issue concerning the behaviors and fates of SPIO nanoparticles-labeled stem cells subjected to an external magnetic field.

II. EXPERIMENTAL METHOD

A. Synthesis of Iron oxide nanoparticles

SPIO nanoparticles were synthesized by the classic chemical coprecipitation method. The technique followed the production process of Ferumoxytol that has been approved by FDA as the inorganic nanodrug. Briefly, PSC (200mg) aqueous solution (10ml) was purged with nitrogen for 5min to remove oxygen. Then, $FeCl_3$ (60mg, 0.37mmol) and $FeCl_2$ (30mg, 0.236mmol) were dissolved in deionized water (15ml). The iron precursor solution was uniformly mixed and added into the PSC solution. Subsequently, 1g ammonium hydroxide (28% w/v) was added into the mixed solution quickly followed by vigorous mechanical stirring under 80℃ water bath for 30 min. Then the iron oxide nanoparticles were collected though ultrafiltration centrifuge tube (30kD) and washed with ultrapure water for several times.

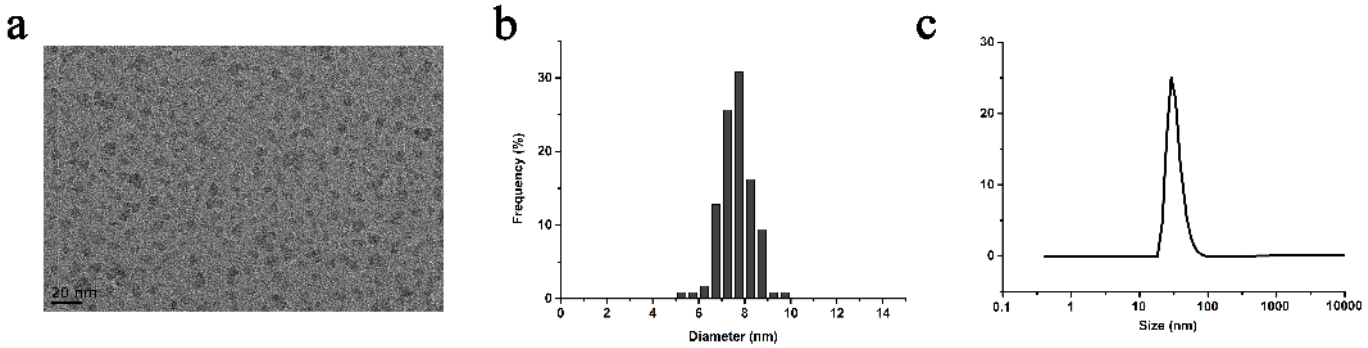

Figure.2 (a) TEM of as-prepared SPIO nanoparticles. (b) The size distribution of nanoparticles in (a). (c) The hydrodynamic size of the the as-prepared SPIO nanoparticle.

Synthesis of Au nanoparticles

As a control, Au NPs were synthesized by a reported method using citric acid as ligands. The prepared Au NPs were purified by centrifugation for at least three times before further use.

B. Cytotoxicity assay

SD-ADMSCs were seeded in 96-well plates at the density of 2×10^5 cells/well and cultured for 12h. The cells were incubated with the treatment of PMF at different frequency and intensity. After incubation for 24h, relative cell viabilities were determined by CCK8 viability assay.

C. Cells counting

SD-ADMSCs were seeded in a 6-well plate (2×10^5 cells/well) for 24h. Then, the cells were typsinized and washed for three times with PBS. After treated with PMF, the washed cells were blocked with 3% BSA solution for 30 min and mixed the cells (10^6 cells/100 μl) with fluorescent-labeled antibodies (0.25μg/l) for 1h at room temperature. The unlabeled cells (control) and antibody-labeled cells were measured by a flow cytometry and the data were analyzed using FlowJo software.

D. Cellular uptake of nanoparticles in the presence of PMF

SD-ADMSCs were seeded in 3.5-cm dishes at the density of 1×10^6 cells/dish and cultured for 12 h for adherence. The cells were taken out from incubator only for PMF treatment. After 24h incubation, the cells were typsinized and washed with PBS for three times, after that the cell counting was carried out using a hemacytometer. Then the cells were centrifuged at 1000g for 5 min, the supernatant was removed and washed with PBS twice. Finally, the cell pellets were lysed by 64% nitric acid on electric furnace for 15min and diluted with deionized water to 5 ml. The iron concentration was determined by inductively coupled plasma optical emission spectrometry (ICP-OES).

E. TEM imaging

SD-ADMSCs were seeded in 96-well plates at the density of 2×10^5 cells/well and cultured for 12 h. After typsinized and washed three times with PBS, the cells were fixed with 2.5% glutaraldehyde in PBS and stored them at 4℃.After dehyrated with ethanol solution in a series of concentrations (20%, 30%, 40%, 50%, 60%, 70%, and 90%), the cell pellets were treated with 2% uranyl acetate in 95% ethanol for 1 h and then dehydrated with 100% ethanol for 1 h. Subsequently, the cell pellets were treated with propylene oxide twice for 15 min and then a mixture of propylene oxide and araldite resin at the volume ratio of 1:1 was prepared. In order to produce ultrathin sections with a microtome, the cells were embedded in araldite resin at 60℃ for 48 h. After that, these slices on copper grids were mounted and stained with 1% aqueous uranyl acetate and 0.2% lead citrate for imaging by TEM (JEM-2000EX, JEOL) at 80 kV acceleration voltage.

III. RESULTS AND DISCUSSIONS

A. PMF generator

The PMF was generated by excitation of coil with pulsed currents, which was schematically shown in **Fig. 1a**. Briefly, the pulsed current was yielded by discharge of large capacitance which switch was controlled by IGBT transistor. In this case the microcontroller was employed to control the switch Q1 and Q2 as was diagramed in **Fig. 1b,** which consist of capacitance charging status and capacitance discharging status. In a complete cycle, the switch Q1 was firstly turned on and the capacitor was quickly charged by the DC power supply. After being fully charged, the switch Q2 was open and the capacitor was quickly discharged to the stimulation coil, thus generating an instantaneous high current pulse in the coil. As the discharge time of stimulation coil drew to an end, the switch Q2 was turned off and the current in the coil is gradually reduced to zero by the return of afterflow. Moreover, details of our designe parameter-adjustable pulsed magnetic field were shown in **Fig. S1**, which displayed the encasement, internal circuit design and coil brace of our parameter-adjustable pulsed magnetic field respectively. The PMF intensity can be controlled by the inductance of coil. When the inductance of load coil was 78μH, the output wave profile was simulated by PLESC software (**Fig. 1c**) and the measured results by current clamp were shown in **Fig. 1d**. It can be seen that the actual output current matched well with that in simulation. The frequency and duty cycle was 5 kHz and 2:1, respectively. The output intensity of PMF was measured by a high-frequency Tesla-meter showing the same case as the current result (**Fig. 1e**). By alteration of the coil inductance and IGBT switch timing, the PMF intensity and frequency can be adjustable in the range of 1.9-4.6mT and 3-5kHz, respectively. In addition, field distribution of PMF was simulated by Ansoft software as was shown in **Fig. S2**, indicating that the PMF was approximately uniform and was suitable for further cellular uptake experiment.

B. Synthesis and characterization of SPIO nanoparticles

The morphology and size of as-prepared SPIO nanoparticles were characterized by TEM (Transmission Electronic Microscopy) and DLS (Dynamic Light Scattering), respectively. The results were shown in **Fig. 2a**. The size of iron oxide cores was about 8nm (**Fig. 2b**) and the hydrodynamic size of the nanoparticles was about 30nm (**Fig. 2c**). Besides, the main parameters of the SPIO nanoparticles were summarized in Supporting Information, **Table S1**. It appears the polydispersity of nanoparticles was good and the nanoparticles were negatively charged. Moreover, the nanoparticles displayed a superparamagnetic hysteresis loop and the saturated magnetization was about 55.57 emu/g at room temperature (Supporting Information, **Fig. S3**). Here, it should be mentioned that the synthesis of our SPIO nanoparticles exactly following techniques of Ferumoxytol that is the only inorganic nanodrug approved by FDA for clinical applications. Importantly, our SPIO nanoparticles have also been approved by CFDA for iron-supplementary and MRI agent, indicating the SPIO nanoparticles we used were of great biosecurity and potentially translatable. Hence, the safety of SPIO nanoparticles as the tracer to label the MSCs is conceivable.

C. Cellular safety assessment of PMF for SD-ADMSCs

SD-ADMSCs cell line was adopted to evaluate the cellular safety of KHz PMF with a standard CCK-8 assay. The KHz PMF, which the frequency was 5 KHz and the intensity was 4.6 mT, was imposed on the cells with two manners. where the frequency was 5 kHz and the intensity was 4.6mT. One was intermittent stimulation, which was to treat the stem cells for three times. The treatment duration per time was dozens of seconds and the interval was 3min. The other was continuous stimulation, which was to treat the cells for over 5min unremittingly. Then the cells were put back to the incubator and tested by CCK8 assay after 24h. The results were shown in **Fig. 3a, b**. For both manners, the PMF showed insignificant damage to the stem cells. The cellular viability exceeded 90% in all investigated conditions. The cellular viability was also confirmed by flow cytometer and the data was in good agreement with test results with CCK8 assay (Supporting Information, **Fig. S4**). Interestingly, it can often be observed that the cells were slightly promoted to grow in the presence of PMF (**Fig. 3c, d**). The cells appeared to be more spreading out and the pseudopods were better visualized. Furthermore, the cell proliferation on 3 days and 7 days post PMF treatment were also evaluated as were shown in Supporting Information **Fig.S5**. It was interesting to see that the PMF with either low or KHz frequency had almost no influence on MSCs.To further illustrate the biosafty of our PMF,we detected the surface markers of MSCs such as CD29, CD11b, CD45 and CD90 (Supporting Information **Fig. S6**). It can be seen that the expression of cell surface markers had rarely changed after PMF treatment, indicating that our PMF scarcely affect the MSCs. we also evaluated the cellular safety of 5Hz and 20 Hz PMF with a standard CCK-8 assay, the result of which was shown in Supporting Information **Fig. S7**. Both 5Hz and 20Hz PMF had almost no damage to the MSCs and the cell viability remained higher than 90%.TEM (Supporting Information **Fig. S8**) and SEM (scanning electron microscopy) (Supporting Information **Fig. S9**) observations also confirmed the morphology had barely changed under the treatment of 5Hz and 20Hz PMF. There have been some reports on the cellular damage of PMF that was of low frequency and high intensity[25][26][27]. However, our PMF was of weak intensity and high frequency. It has been extensively recognized that the alternating magnetic field of kHz range is biologically safe[28][29]. This case may account for the safety of our PMF.

D. Entry of SPIO nanoparticles into SD-ADMSCs in the presence of PMF

Cellular uptake of SPIO nanoparticles was quantitatively measured by using ICP-OES. Firstly, the iron content of SD-ADMSCs without any treatment has been measured and the value was 0.31±0.02 pg/cell, which was too small to be taken into account and the value was consistent with our previous study[30]. Surprisingly, the cellular uptake of SPIO nanoparticles was greatly prohibited in the presence of PMF of 5kHz and this was also the case for the 3kHz PMF (**Fig. 4a, b**). This phenomenon was opposite from the common reports. We thought this may result from the relatively high frequency of PMF. Then we used the 5Hz and 20Hz PMF to repeat this experiment, and found that the entry of SPIO nanoparticles into the stem cells was significantly promoted, in agreement with the previous reports (**Fig. 4c, d**). Moreover, it was discovered that for the 5Hz and 20Hz PMF, the intracellular Fe content was significantly increased depending on the treatment duration. However, the intracellular Fe content showed nearly constant with the extension of treatment duration for the 3kHz PMF. For the 5kHz PMF, although the intracellular Fe content showed an increasing tendency after the treatment duration exceeded 10min, the increment was insignificant.

The influence of PMF intensity was also investigated. The field intensities were 1.9mT, 2.6mT and 3.5mT, respectively. Here, the field frequency was fixed at 5kHz. It was found that the intracellular Fe content was significantly reduced with the increase of the PMF intensity regardless of the intermittent mode or the continuous mode (**Fig. 5a-f**). Furthermore, the higher field intensity showed greater prohibition effect upon the cellular uptake of SPIO nanoparticles. The quantitative evaluation demonstrated that the reduction of intracellular Fe content shifted from 78.1±6.8% at 1.9mT to 58.3±6.6% at 3.5mT (Supporting Information, **Fig. S10)**.

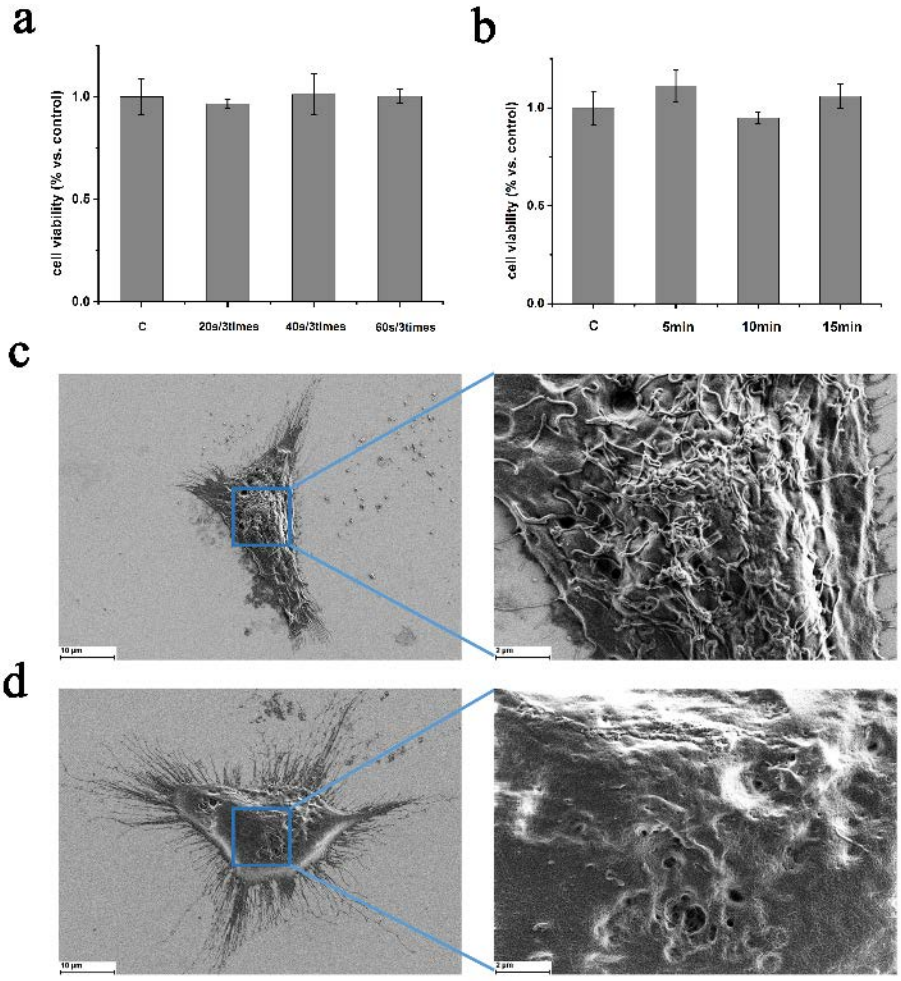

Figure.3 (a-b) Cell viability of SD-ADSCs after treated with PMF by a standard CCK-8 assay at intermittent and continuous stimulus parameter respectively. (c-d) The morphology of SD-ADSCs without and with the PMF treatment respectively.

The intracellular distribution of SPIO nanoparticles was also characterized by TEM. It was seen that the nanoparticles were packed within vesicles in the absence of the PMF (**Fig. 5g**), where the nanoparticles presented in the form of aggregation. It should be mentioned that the hydrodynamic size by the DLS (Supporting Information, **Fig. S11)** had not changed under the treatment of PMF, indicating that the PMF cannot cause the SPIO aggregated. This is the common case for the entry of nanoparticles into the cells because of the clathrin-dependent endocytosis pathway. The terminal fate is to be degraded in the lysosomes of cells by various of hydrolytic enzymes such as the lysosomal cathepsin L[31]. Besides, the degradation of SPIO nanoparticles within MSCs had been quantified at the single-cell level and gave strong evidence to the possible synthesis of magnetic nanoparticles in cellulo linked to an excess of iron delivered by nanoparticles degradation[32]. Generally, the mechanism of the transmembrane entry of SPIO nanoparticles into the cells lie in the clathrin mediated endocytosis, where the nanoparticles was enveloped by vesicle and finally degradated in lysosomes[33]. When treated with KHz-ranged PMF, the cells are subjected to magnetic force and the SPIO nanoparticles can directly enter the cells, thus preventing the degradation by lysosomes. As expected, after the treatment of PMF, the nanoparticles were found to locate in the cytoplasm without packing by vesicles (**Fig. 5h**). Moreover, the morphology of the stem cells became rough after the treatment with the PMF (Supporting Information, **Fig. S12)**. The rough interface may obstruct the entry of the SPIO nanoparticles into cells because the curvous morphology can counteract the potential energy of hard particles to prohibit deformation of cellular membrane[34][35][36]. We thought that when treated with Hz-ranged PMF, the cells are subjected to magnetic force, which might open some channels on the cell membrane and the uptake of SPIO nanoparticles by MSCs was significantly promoted. While treated with KHz-ranged PMF, the cell membrane turn rough under the continuous stimulation, thus hindering the cellular internalization. In addition, magnetic thermogenesis of SPIO nanoparticles was also measured under the treatment of 3KHz PMF with an optical thermometer and the result was shown in Supporting Information, **Fig. S13,** where it can be seen that there was scarce magnetic hyperthermia effects, which had no role in internalization inhibition. Dark field scattering microscopy was used to investigate the distribution of SPIO nanoparticles. The small particles can yield strong side scattering under the eclipse mode of laser confocal microscopy so that a small cluster of nanoparticles was presented as a lightspot. The lightspots can be quantitatively calculated to reflect the amount of SPIO nanoparticles in the cells. Here, it

should be mentioned that the larger lightspot represents the bigger aggregates of nanoparticles because the scattering intensity is proportional to the size of objects. The results were shown in Supporting Information, **Fig. S14**. The statistical results revealed that the PMF significantly prohibit the entry of nanoparticles into the cells. Of more interests, the co-incubation of nanoparticles and the cells demonstrated the larger lightspots indicating that the nanoparticles formed the aggregates inside after entry into the cells. However, the lightspots were uniform and dispersed over the PMF-treated nanoparticles and cells. This case means that the nanoparticles were distributed uniformly and dispersively, partly validating the results of TEM.

Compared with the magnetostatic field and the field of extremely low frequency, the induction electrical field of our PMF should not be neglected. Here, Au nanoparticles were employed to demonstrate the role of induction electrical field because the Au nanoparticles owned the nearly identical size compared to the SPIO nanoparticles but without the superparamagnetism. The uptake of Au nanoparticles by the stem cells was investigated in the presence of the PMF of 3/5kHz and the PMF of 5/10Hz (Supporting Information, **Fig. S15**). It was shown that the PMF treatment had neglectable influence upon the cellular uptake of Au nanoparticles. The amount of Au element showed almost no difference in the presence of both PMFs. It validated the prohibition effect of PMF did not result from the induction of electric field.

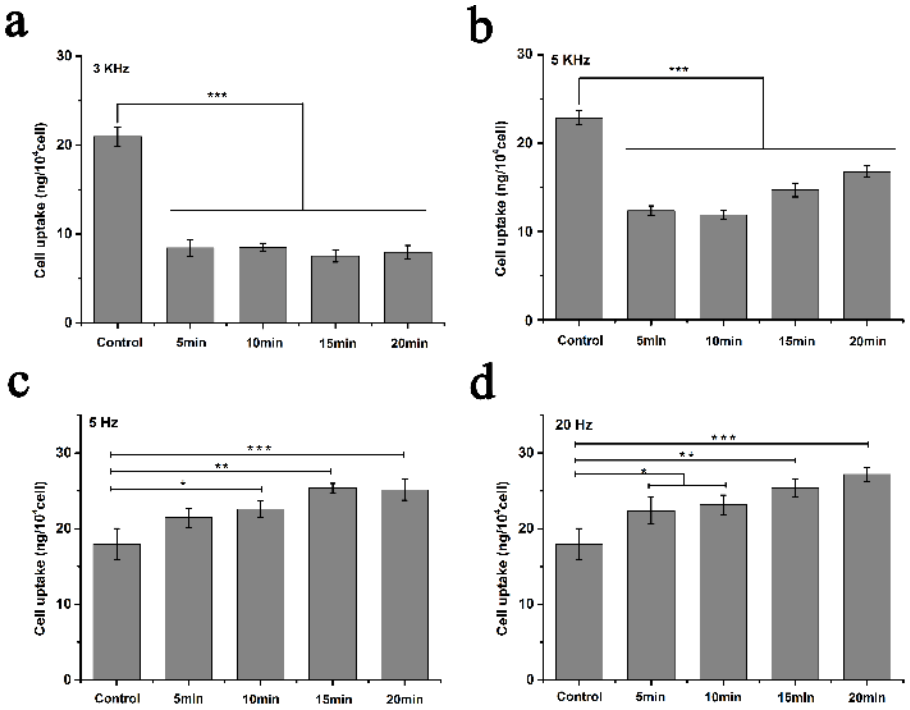

Figure.4 (a-b) The cellular uptake of SPIO nanoparticles with the treatment of PMF of 3kHz and 5KHz respectively. (c-d) The cellular uptake of SPIO nanoparticles with the treatment of PMF of 5Hz and 20Hz respectively. Asterisk indicates statistically significant differences between control and experience group (* $0.01< p < 0.05$, ** $0.001< p < 0.01$, *** $p < 0.001$,). Student t-test was used to assess significant differences.

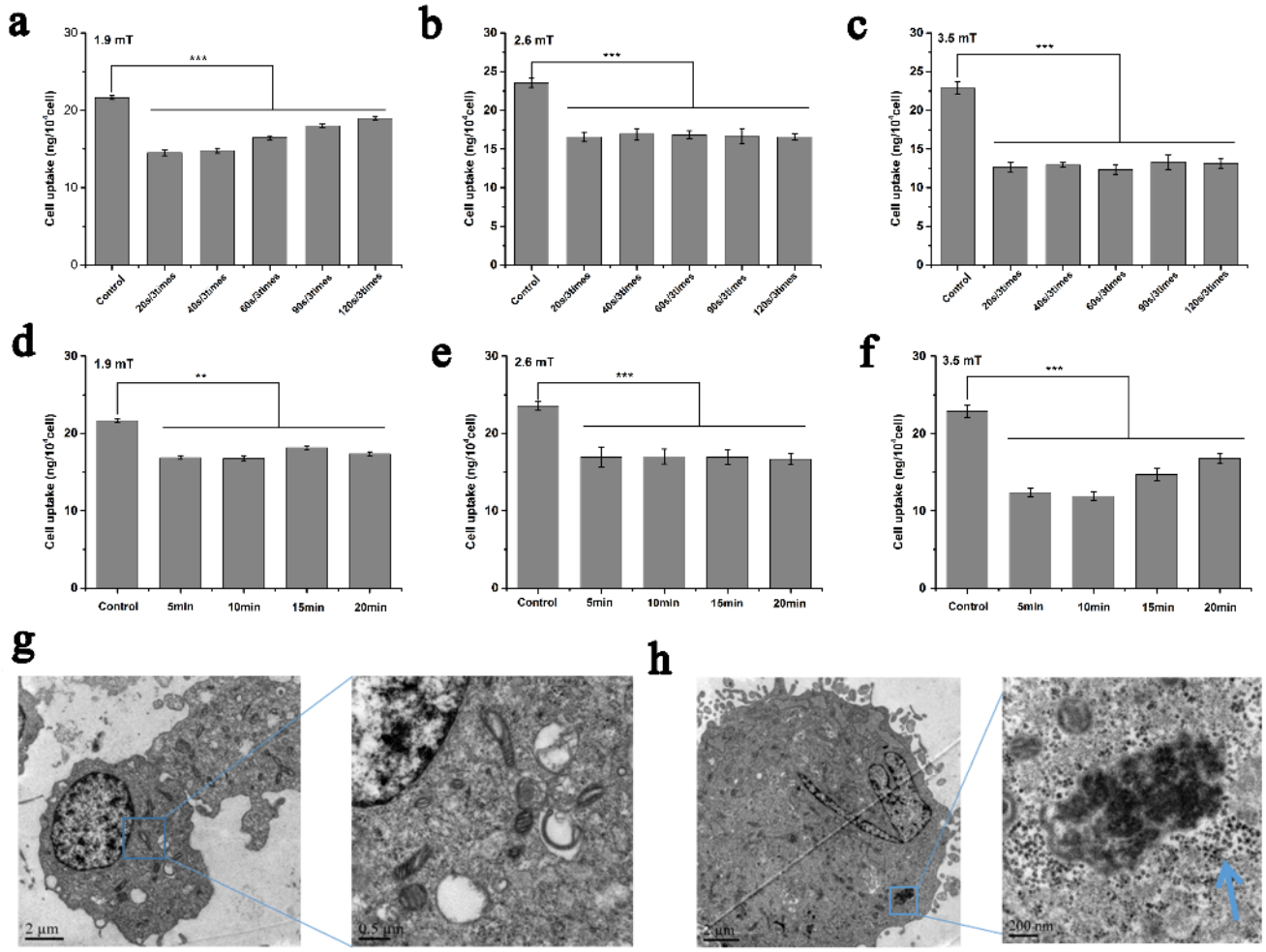

Figure.5 (a-c) The intracellular Fe content with the AMF of 1.9mT, 2.6mT and 3.5mT intensity of the intermittent mode respectively. (d-f) The intracellular Fe content with the AMF of 1.9mT, 2.6mT and 3.5mT intensity of the continuous mode respectively. (g-h) Transmission electron microscopy of cell uptake of SPIO nanoparticles by SD-ADSCs without and with the treatment of PMF respectively. Asterisk indicates statistically significant differences between control and experience group (*** $p < 0.001$,). Student t-test was used to assess significant differences.

IV. CONCLUSION

In conclusion, we produced a pulsed magnetic field (PMF) which intensity and frequency were 1.9-4.6mT and 3-5kHz, respectively. This kHz-ranged PMF was discovered to significantly prohibit the uptake of SPIO nanoparticles by SD-ADMSCs. However, the PMF of several Hz can promote the cellular uptake of SPIO nanoparticles. By control experiments with Au nanoparticles, the influence from the induction of electric field was excluded. These results demonstrated that the entry of SPIO nanoparticles into the stem cells can be regulated by the external magnetic field. Considering the extensive application of SPIO nanoparticles in research fields of stem cells in which the magnetic field has often been involved, this novel phenomenon will play a promising role in regenerative medicine and regulation of stem cells.

Copyright

REFERENCES

[1] A Trounson et al. “Stem Cell Therapies in Clinical Trials: Progress and Challenges”, Cell Stem Cell, vol.17(1), pp.11-22, Jul., 2015.

[2] J M Karp et al. “Mesenchymal Stem Cell Homing: The Devil Is in the Details”, Cell Stem Cell, vol.4(3), pp.206-216, Mar., 2009

[3] M J Dalby et al. “Receptor control in mesenchymal stem cell engineering”, Nature Reviews Materials, vol.3(3), Jan., 2018.

[4] Q Chen et al. “Fate decision of mesenchymal stem cells: adipocytes or osteoblasts?” Cell Death and Differentiation, vol.23(7), pp.1128-1139, Feb., 2016.

[5] P Keselman et al. “Tracking short-term biodistribution and long-term clearance of SPIO tracers in magnetic particle imaging”, Physics in Medicine and Biology, vol.62(9), pp.3440-3453, May., 2017.

[6] M R Bashir et al. “Emerging Applications for Ferumoxytol as a Contrast Agent in MRI”, Journal of Magnetic Resonance Imaging, vol.41(4), pp.884-898, Apr., 2015.
[7] F G Fan et al. “Rotating magnetic field-controlled fabrication of magnetic hydrogel with spatially disk-like microstructures”, Science China Materials, vol.61(8), pp.1112-1122, Aug., 2018.
[8] C H Fan et al.“Ultrasound/Magnetic Targeting with SPIO-DOX-Microbubble Complex for Image-Guided Drug Delivery in Brain Tumors”, Theranostics, vol.6(10), pp.1542-1556, Jun., 2016.
[9] Y Xu et al. “Superparamagnetic MRI probes for in vivo tracking of dendritic cell migration with a clinical 3 T scanner”, Biomaterials, vol.64(58), pp.63-71, Jul., 2015.
[10] D Romero. “Tracing stem cells in oligodendroglioma”, Nature Reviews Clinical Oncology, vol.14(1), pp.2-2, Jan., 2017.
[11] E U Saritas et al. “Magnetic Particle Imaging (MPI) for NMR and MRI researchers”. Journal of Magnetic Resonance, vol.229, pp.116-126, Nov., 2013.
[12] K Unfried et al. “Cellular responses to nanoparticles: Target structures and mechanisms”, Nanotoxicology, vol.1(1) pp.52-71, Jan., 2007.
[13] Q Wang et al. “Response of MAPK pathway to iron oxide nanoparticles in vitro treatment promotes osteogenic differentiation of hBMSCs”, Biomaterials, vol.86, pp.11–20, Apr., 2016.
[14] Q Wang et al. “Magnetic iron oxide nanoparticles accelerate osteogenic differentiation of mesenchymal stem cells via modulation of long noncoding RNAINZEB2”, Nano Research, vol.10(2), pp.626-642, Apr., 2017.
[15] L Kostura et al. “Feridex labeling of mesenchymal stem cells inhibits chondrogenesis but not adipogenesis or osteogenesis”, NMR in Biomedicine, vol. 17(7), pp.513-517, Nov., 2004.
[16] R Emilie et al. “Dose-Response of Superparamagnetic Iron Oxide Labeling on Mesenchymal Stem Cells Chondrogenic Differentiation: A Multi-Scale In Vitro Study”, PLOS ONE, vol.9(5), pp.98451-98460, May., 2014.
[17] Du V et al. “A 3D magnetic tissue stretcher for remote mechanical control of embryonic stem cell differentiation”, Nature Communications, vol.8(1), pp.400-411, Sep., 2017.
[18] C A M Smith et al. “The effect of static magnetic fields and tat peptides on cellular and nuclear uptake of magnetic nanoparticles”, Biomaterials, vol.31(15), pp.4392-4400, May.,2010.
[19] Q Liu et al. “Towards magnetic-enhanced cellular uptake, MRI and chemotherapeutics delivery by magnetic mesoporous silica nanoparticles”. J Nanosci Nanotechnol, vol.12(10), pp.7709-7715,Oct., 2012.
[20] C H Lee et al. “Cellular uptake of protein-bound magnetic nanoparticles in pulsed magnetic field”. J Nanosci Nanotechnol, vol.10(12), pp.7965-7970, Dec., 2010.
[21] M Uzhytchak et al. “The use of pulsed magnetic fields to increase the uptake of iron oxide nanoparticles by living cells.” Applied Physics Letters, vol.111(24), pp.243703, Dec.,2017.
[22] J N PHILLIPS et al. “Electromagnetic fields and DNA damage”, Pathophysiology, vol.16(2), pp.79-88, 2009.
[23] R P LIBURDY. “Cellular studies and interaction mechanisms of extremely low frequency fields”, Radio Science, vol.30(1), pp.179-203, Jan.,1995.
[24] C S Poon et al. “Transient response studies of biological cell impedance”， Medical & Biological Engineering & Computing, vol.16(6), pp.633-641, Nov., 1978.
[25] J Y Qian et al. “Proteomics Analyses and Morphological Structure of Bacillus subtilisInactivated by Pulsed Magnetic Field”, Food Biophysics, vol.11(4), pp.436-445, Dec., 2016.
[26] J Y Qian et al. “Biological Effect and Inactivation Mechanism ofBacillus subtilisExposed to Pulsed Magnetic Field: Morphology, Membrane Permeability and Intracellular Contents”, Food Biophysics, vol.11(4), pp.429-435, Dec., 2016.
[27] P Solek et al. “Pulsed or continuous electromagnetic field induce p53/p21-mediated apoptotic signaling pathway in mouse spermatogenic cells, in vitro, and thus may affect male fertility”, Toxicology, vol.382, pp.84-92, Mar., 2017.
[28] L F Rapha et al. “Enhanced antitumor efficacy of biocompatible magnetosomes for the magnetic hyperthermia treatment of glioblastoma”, Theranostics, vol. 18(7), pp.4618-4631, Oct., 2017.
[29] A Sathya et al. “One-step Microwave-assisted Synthesis of Water-dispersible Fe_3O_4 Magnetic Nanoclusters for Hyperthermia Applications”, Journal of Magnetism and Magnetic Materials, vol.439, pp.109-117, Oct.,2017.
[30] Y Yan et al. “Uptake of magnetic nanoparticles for adipose-derived stem cells with multiple passage numbers.” science china materials, vol.60(9), pp. 892-902, Sep., 2017.
[31] Laskar A, et al. “Degradation of superparamagnetic iron oxide nanoparticle-induced ferritin by lysosomal cathepsins and related immune response”, Nanomedicine, vol.7, pp.705–717, Mar., 2012.
[32] Van de Walle A et al. “Biosynthesis of magnetic nanoparticles from nano-degradation products revealed in human stem cells”, PNAS, vol.116(10), pp.4044-4053, Feb., 2019.
[33] S L Zhang et al. “Physical Principles of Nanoparticle Cellular Endocytosis”, Acs Nano, vol.9(9), pp.8655-8671, Aug., 2015.
[34] P Zhao et al. “Downregulation of MIM protein inhibits the cellular endocytosis process of magnetic nanoparticles in macrophages.” RSC Adv, vol.99(6), pp.96635–96643, 2016.
[35] da Luz CM et al. “Poly-lactic acid nanoparticles (PLA-NP) promote physiological modifications in lung epithelial cells and are internalized by clathrin-coated pits and lipid rafts”, J Nanobiotechnol, vol.15(1), pp.11–29, Jan., 2017.
[36] A Banerjee et al. “Kinetics of cellular uptake of viruses and nanoparticles via clathrin-mediated endocytosis.” Phys Biol, 2016, 13(1), pp.016005, Feb., 2016.